

# Utilizing Generative Adversarial Networks for Image Data Augmentation and Classification of Semiconductor Wafer Dicing Induced Defects

Zhining Hu<sup>1,\*</sup>, Tobias Schlosser<sup>1,\*</sup>, Michael Friedrich<sup>1,\*</sup>,

André Luiz Vieira e Silva<sup>2</sup>, Frederik Beuth<sup>1</sup>, and Danny Kowerko<sup>1</sup>

<sup>1</sup>Junior Professorship of Media Computing, Chemnitz University of Technology, 09107 Chemnitz, Germany

<sup>2</sup>Voxar Labs, Centro de Informática, Universidade Federal de Pernambuco, Brazil

\*Zhining Hu, Tobias Schlosser, and Michael Friedrich contributed equally to this work

{firstname.lastname}@cs.tu-chemnitz.de

**Abstract**—In semiconductor manufacturing, the wafer dicing process is central yet vulnerable to defects that significantly impair yield – the proportion of defect-free chips. Deep neural networks are the current state of the art in (semi-)automated visual inspection. However, they are notoriously known to require a particularly large amount of data for model training. To address these challenges, we explore the application of generative adversarial networks (GAN) for image data augmentation and classification of semiconductor wafer dicing induced defects to enhance the variety and balance of training data for visual inspection systems. With this approach, synthetic yet realistic images are generated that mimic real-world dicing defects. We employ three different GAN variants for high-resolution image synthesis: Deep Convolutional GAN (DCGAN), CycleGAN, and StyleGAN3. Our work-in-progress results demonstrate that improved classification accuracies can be obtained, showing an average improvement of up to 23.1 % from 65.1 % (baseline experiment) to 88.2 % (DCGAN experiment) in balanced accuracy, which may enable yield optimization in production.

**Index Terms**—Computer Vision, Pattern Recognition, Visual Inspection, Data Synthesis, Deep Learning, Convolutional Neural Networks

## I. INTRODUCTION AND MOTIVATION

Semiconductors, materials with electrical conductivity between conductors and insulators, are crucial for integrated circuits or chips, used in numerous electronic products. The global semiconductor market is projected to reach \$588.36 billion in 2024, highlighting the sector’s economic significance and the growing global focus on semiconductor manufacturing [1]. The industry, characterized by high technical costs, emphasizes quality control and yield optimization – the ratio of flawless to total chips produced post-dicing [2]. The semiconductor wafer dicing process is a critical manufacturing step that involves complex procedures where defects within the dicing streets – separations created during chip dicing – significantly impact the chips’ quality (Fig. 1) [3]. Various defect patterns can arise from machine errors or human error, necessitating robust defect detection and classification systems to maintain yield [4].

Traditional defect detection methods include manual inspections and contact needle tests, which are especially time-

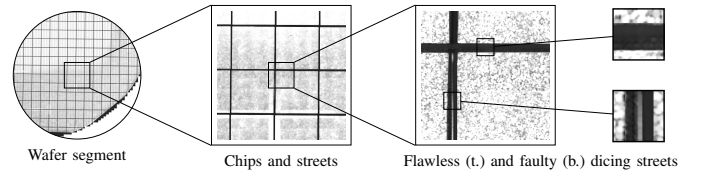


Figure 1: Wafer overview with chips and dicing streets (reprinted and adapted from [5], copyright IEEE).

consuming, potentially inaccurate, or can damage the wafer [6]. Advances in artificial intelligence (AI), particularly machine learning (ML) and deep learning (DL), have led to the development of (semi-)automated visual inspection systems that offer an effective solution for identifying and classifying dicing street defects [4]. However, deep neural networks (DNN) are notoriously known for requiring a significant amount of data to be trained successfully. To complicate matters further, data samples must be available for all types of defects (denoted as class defects). For example, the popular ImageNet data set contains 1 000 sample images for each object type (class). However, in industry applications, obtaining such a magnitude of defect images is very challenging. Thus, despite technological advances, data scarcity and imbalance in wafer image data remain major difficulties. The industry’s reliance on proprietary rights and significant barriers to entry hinder the acquisition of high-quality, labeled data sets comparable to those in other fields [7], [8], further hindering research and development within the field. To overcome these challenges, data augmentation techniques such as geometric transformations, noise injection, and the use of generative adversarial networks have been employed. GANs [9], in particular, have shown promising results for a wide variety of application areas by generating high-quality synthetic images to enhance the performance and generalization capabilities of learning-based classification models [10]. This includes novel applications of image super-resolution, medical image synthesis, protein structure generation, and astronomical image simulation [11].

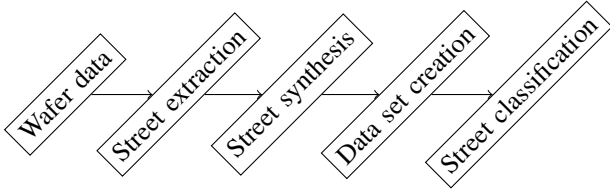


Figure 2: Designed visual fault synthesis and inspection system for dicing street generation and classification.

Table I: Data set overview with wafer types, number of streets, and widths and image resolutions of the dicing streets [4].

Wafer type	1	2	3	4	5
Streets	4 436	13 504	7 024	428	2 368
Flawless Streets	3 983	12 624	6 891	297	2 094
Faulty Streets	453	880	133	131	274
Street width [px]	15 or 25	4	20	19	23
Street image resolution [px]	$379 \times 56$	$384 \times 36$	$372 \times 51$	$378 \times 44$	$374 \times 62$

To address data imbalance and scarcity in training learning-based models for (semi-)automated visual inspection in semiconductor wafer dicing, this contribution introduces a data augmentation methodology that utilizes GANs. This involves selecting a set of suitable GAN models, their training on existing dicing street imagery, and using them to enhance the original data set with generated images to create an extended and balanced hybrid data set. This extended data set is then used to train our classification model. The possible benefits of this approach in terms of classification capabilities are demonstrated by our results, which align with our previous works in the field of semiconductor wafer data sets, such as *Schlosser et al.* [4].

## II. FUNDAMENTALS AND IMPLEMENTATION

### A. Generative adversarial networks

GANs are based on a two-player zero-sum game involving a generator and a discriminator in a min-max optimization setup. The generator aims to produce data mimicking a true distribution to fool the discriminator, whereas the discriminator tries to distinguish between generated and real samples. This methodology elevates GANs in generating complex, high-quality data, which has been transformative across various data augmentation applications [12].

*Radford et al.* (2016) [13] introduced deep convolutional GANs, which combine convolutional neural networks (CNN) with GANs, improving sample quality and training stability.

Table II: Overview of our experimental configurations for our evaluation with experiment IDs 1 to 3.

Experiment ID	Training set	Test set	Oversampling?
1 (Baseline)	Original train set	Original test set	No
2 (Oversampling)	Baseline, balanced via oversampling	Original test set	Yes
3	3.1 DCGAN	Original test set	No
	3.2 CycleGAN		
	3.3 StyleGAN3		

DCGANs have been effectively applied in fields including pedestrian recognition and medical image classification, significantly increasing model accuracy and diagnostic precision [14], [15]. In comparison, CycleGAN (2017) [16] facilitates image-to-image translation tasks without needing paired samples, which simplifies training data preparation. CycleGANs have proven effective in style transfer, medical imaging, and even in generating facial expressions or remote sensing images, demonstrating their utility in domain adaptation [17], [18]. The introduction of StyleGAN by *Karras et al.* (2019) [19] optimized the GAN architecture for generating high-resolution images, which is crucial for tasks requiring detailed visual fidelity such as medical imaging or object detection. StyleGAN uses adaptive instance normalization and a novel style-based loss function to refine image quality progressively from low to high resolution, enhancing the realism of generated images and thereby the effectiveness of data augmentation [20], [21]. With its most recent version, StyleGAN3 (2021) [22], *Karras et al.* further optimized the architecture and training efficiency, effectively addressing aliasing issues within the generator network. However, GANs are not universally applicable. They require substantial initial data for effective training and can suffer from training instabilities.

### B. Designed system

Fig. 2 details our designed system for wafer-based street extraction and synthesis, data set creation, and street classification, for which the semiconductor wafer dicing data set summarized in Table I is deployed. For the synthesis of street imagery, our implementation includes three GAN variants, DCGAN, CycleGAN, and StyleGAN3, which are trained with minimal initial parameter tuning as out-of-the-box models. All street images were scaled to an image resolution of  $192 \times 64$  pixels. Subsequently, we mainly follow the methodology of our previous work of *Schlosser et al.* (2022) [4], whereby cuttings of the chips (streets) are fed to a DNN for street classification, simulating a process of focusing on relevant chip regions via visual attention as shown by *Beuth et al.* (2021) [23]. For classification, the residual neural network ResNet152V2 [24] is employed as classification model to obtain classification results comparable to [4]. Our implementations leverage Python with PyTorch for image generation, whereas the Hexnet framework [25] is deployed for image classification.

## III. TEST RESULTS, EVALUATION, AND DISCUSSION

### A. Data sets and experimental configurations

Table I details the baseline data set used within this contribution. Initially, the data set of dicing street samples is split, allocating 80 % to form the original training set (of which 10 % form our validation set), with the remaining 20 % forming the original test set. The original data sets function as our reference for creating hybrid data sets. In addition, our test sets exclusively consist of original data for all experiments. Here, the inclusion of generated faulty samples in the original training sets facilitates the creation of balanced hybrid data sets.

Table III: Overview of our original and generated flawless and faulty street samples per wafer type.









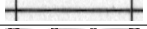
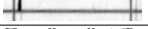
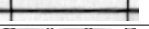
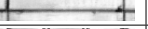
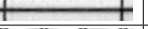
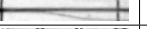
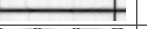
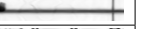
























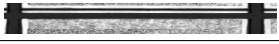


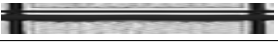




















Wafer type	Original		DCGAN		CycleGAN		StyleGAN3	
	Flawless	Faulty	Flawless	Faulty	Flawless	Faulty	Flawless	Faulty
1								
2								
3								
4								
5								

Table IV: Overview of different faulty street classes that have been generated per wafer type.

Error type	Original	DCGAN	CycleGAN	StyleGAN3
Chip excess				
Undersize				
Nose				
Chipping				
Wafer border				
Imaging error				

Three experimental configurations have been established to evaluate the efficiency of different data balancing strategies on classification performance (Table II). (1) Baseline experiment. Does not utilize any data balancing techniques. (2) Oversampling experiment. The impact of class balancing within the training set is tested by sample duplication. This configuration aims to determine the effectiveness of data oversampling. (3) Hybrid experimental configuration, in which GANs are employed for training data generation within the training set. This configuration is subdivided via our three GAN variants, DCGAN, CycleGAN, and StyleGAN3.

## B. Results

Similar to [4], our proposed ResNet152V2-based training setup included the following: the Glorot initializer for weight initialization, the Adam optimizer with a standard learning rate of 0.001 and exponential decay rates of 0.9 and 0.999, as well as a batch size of 32. Training was performed over 20 epochs, for which the results of five training runs were assessed. We used the balanced accuracy and unbalanced weighted F1-score as metrics. The generated samples per model and occurring defect classes are shown in Tables III and IV. Our key findings are summarized in Table V.

1) *Impact of data balancing on model performance:* Oversampling: Traditional oversampling has shown limited effectiveness as evidenced by minor improvements across all wafer types. Hybrid balancing: GANs for data augmentation can significantly enhance the classification performance, surpassing the results achieved with oversampling. Averaged over all five wafers, our best result was obtained in experiment 3.1 with DCGAN, showing an improvement of up to 23.1 % from 65.1 % (experiment ID 1, baseline) to 88.2 % (experiment ID 3.1 with DCGAN) in balanced accuracy.

2) *Comparative analysis of GAN architectures:* Our experiments highlight the increased performance of DCGAN and CycleGAN over StyleGAN3, with DCGAN outperforming

CycleGAN. Therefore, DCGAN is recommended for practical implementation because of its potentially lower computational demands and faster training times, making it more cost-effective for large-scale applications.

3) *Effectiveness across different wafer types:* Varied responses to GAN-based data augmentation were observed among different wafer types. Wafer types 3 and 4 showed the most significant improvement in balanced accuracy. In contrast, wafer types 1 and 2 exhibited in turn fewer improvements. These findings emphasize a correlation between the effectiveness of data augmentation strategies and the initial data sets' size (Table I). Analyzing this correlation, GANs seem to yield the best results when only a reduced number of faulty or total samples are provided within the original data set. This is evident from the notable improvement observed in wafer type 4 (428 total samples, 131 faulty class samples) and wafer type 3 (7024 total samples, yet only 133 faulty class samples).

## IV. CONCLUSION AND OUTLOOK

Our work-in-progress results confirm that generative adversarial networks are a viable solution to the prevalent challenges of data scarcity and imbalance in semiconductor manufacturing for semiconductor wafer dicing. By generating synthetic yet realistic image data sets, GANs can improve the classification capabilities of deep learning models by enhancing defect detection accuracies. All three studied GAN architectures offer advantages over our baseline experiments. DCGAN offers slight advantages over CycleGAN and StyleGAN3. Therefore, DCGAN is our recommendation due to its efficiency and potentially lower operational costs.

This research not only aimed at advancing the understanding of GAN applications in industrial settings, but also aimed to set a benchmark for future studies aiming to optimize data-intensive inspection processes within semiconductor wafer dicing. For this purpose, unified image resolutions per wafer



Table V: Overview of the results obtained from our three experimental configurations described in Table II based on the street data sets displayed in Table III. Shown are the results over five test runs in balanced accuracy (BA) and weighted F1-score (F1) [%] per experiment. Color-coded scores emphasize the change in classification performance from the oversampling experiment (exp. 2): **green** and **red** highlight increased and decreased scores. The best overall results are highlighted in bold.

Experiment ID	Wafer type 1				Wafer type 2				Wafer type 3				Wafer type 4				Wafer type 5				Average				
	BA		F1		BA		F1		BA		F1		BA		F1		BA		F1		BA		F1		
1 (Baseline)	76.2 ± 8.9	86.0 ± 4.9	73.5 ± 2.9	85.1 ± 12.3	53.9 ± 2.6	92.6 ± 0.6	55.4 ± 9.8	42.8 ± 15.9	66.7 ± 2.1	81.4 ± 1.5	65.1 ± 5.3	77.6 ± 7.0	81.4 ± 2.4	89.9 ± 1.0	83.6 ± 3.8	89.5 ± 8.4	57.0 ± 8.3	92.7 ± 1.1	64.8 ± 13.3	58.2 ± 20.9	67.0 ± 1.5	81.6 ± 0.9	70.8 ± 5.9	82.4 ± 6.5	
2 (Oversampling)	81.4 ± 2.4	89.9 ± 1.0	83.6 ± 3.8	89.5 ± 8.4	57.0 ± 8.3	92.7 ± 1.1	64.8 ± 13.3	58.2 ± 20.9	67.0 ± 1.5	81.6 ± 0.9	70.8 ± 5.9	82.4 ± 6.5	81.4 ± 2.4	89.9 ± 1.0	83.6 ± 3.8	89.5 ± 8.4	57.0 ± 8.3	92.7 ± 1.1	64.8 ± 13.3	58.2 ± 20.9	67.0 ± 1.5	81.6 ± 0.9	70.8 ± 5.9	82.4 ± 6.5	
3	3.1 DCGAN	92.9 ± 2.8	94.3 ± 3.4	88.1 ± 4.3	95.1 ± 0.9	80.5 ± 9.9	96.2 ± 1.2	92.9 ± 7.9	92.7 ± 8.5	86.6 ± 9.7	93.0 ± 5.3	88.2 ± 6.9	94.3 ± 3.9	89.6 ± 4.6	90.8 ± 6.0	86.8 ± 3.3	91.0 ± 7.0	82.0 ± 11.5	94.8 ± 4.0	86.7 ± 14.1	85.1 ± 16.8	81.8 ± 11.7	89.7 ± 6.3	85.4 ± 9.0	90.3 ± 8.0
	3.2 CycleGAN	89.6 ± 2.6	90.8 ± 6.0	86.8 ± 3.3	91.0 ± 7.0	82.0 ± 11.5	94.8 ± 4.0	86.7 ± 14.1	85.1 ± 16.8	81.8 ± 11.7	89.7 ± 6.3	85.4 ± 9.0	90.3 ± 8.0	80.0 ± 14.4	75.5 ± 29.5	90.9 ± 4.2	96.1 ± 0.7	79.3 ± 5.8	94.8 ± 4.1	81.7 ± 20.0	77.7 ± 25.9	86.9 ± 5.3	90.9 ± 5.7	83.8 ± 9.9	87.0 ± 13.2
	3.3 StyleGAN3	80.0 ± 14.4	75.5 ± 29.5	90.9 ± 4.2	96.1 ± 0.7	79.3 ± 5.8	94.8 ± 4.1	81.7 ± 20.0	77.7 ± 25.9	86.9 ± 5.3	90.9 ± 5.7	83.8 ± 9.9	87.0 ± 13.2	80.0 ± 14.4	75.5 ± 29.5	90.9 ± 4.2	96.1 ± 0.7	79.3 ± 5.8	94.8 ± 4.1	81.7 ± 20.0	77.7 ± 25.9	86.9 ± 5.3	90.9 ± 5.7	83.8 ± 9.9	87.0 ± 13.2

type should be generated to allow the combination of different wafer types within one data set. Future work should also explore the integration of hybrid data augmentation strategies that combine the strengths of different GAN architectures and further refine the balance between computational efficiency and model performance. Expanding the scope to include more diverse wafer types and defect categories could unveil further insights into the scalability and adaptability of GAN-based data augmentation within this domain.

#### ACKNOWLEDGMENT

The European Union via the European Social Fund for Germany partially funded this research (grant number 100670286).

#### REFERENCES

- [1] Statista (May 26, 2024)., “Semiconductor market revenue worldwide from 1987 to 2024 [Online].” <https://www.statista.com/statistics/266973/global-semiconductor-sales-since-1988/>.
- [2] K. B. Lee, S. Cheon, and C. O. Kim, “A Convolutional Neural Network for Fault Classification and Diagnosis in Semiconductor Manufacturing Processes,” *IEEE Transactions on Semiconductor Manufacturing*, vol. 30, no. 2, pp. 135–142, May 2017.
- [3] S.-H. Huang and Y.-C. Pan, “Automated visual inspection in the semiconductor industry: A survey,” *Computers in Industry*, vol. 66, pp. 1–10, Jan. 2015.
- [4] T. Schlosser, M. Friedrich, F. Beuth, and D. Kowanko, “Improving automated visual fault inspection for semiconductor manufacturing using a hybrid multistage system of deep neural networks,” *Journal of Intelligent Manufacturing*, vol. 33, no. 4, pp. 1099–1123, Apr. 2022.
- [5] T. Schlosser, F. Beuth, M. Friedrich, and D. Kowanko, “A Novel Visual Fault Detection and Classification System for Semiconductor Manufacturing Using Stacked Hybrid Convolutional Neural Networks,” in *2019 24th IEEE International Conference on Emerging Technologies and Factory Automation (ETFA)*, Sep. 2019, pp. 1511–1514.
- [6] K. C.-C. Cheng, L. L.-Y. Chen, J.-W. Li, K. S.-M. Li, N. C.-Y. Tsai, S.-J. Wang, A. Y.-A. Huang, L. Chou, C.-S. Lee, J. E. Chen, H.-C. Liang, and C.-L. Hsu, “Machine Learning-Based Detection Method for Wafer Test Induced Defects,” *IEEE Transactions on Semiconductor Manufacturing*, vol. 34, no. 2, pp. 161–167, May 2021.
- [7] L. Deng, “The MNIST Database of Handwritten Digit Images for Machine Learning Research [Best of the Web],” *IEEE Signal Processing Magazine*, vol. 29, no. 6, pp. 141–142, Nov. 2012.
- [8] J. Deng, W. Dong, R. Socher, L.-J. Li, K. Li, and L. Fei-Fei, “ImageNet: A large-scale hierarchical image database,” in *2009 IEEE Conference on Computer Vision and Pattern Recognition*, Jun. 2009, pp. 248–255.
- [9] I. J. Goodfellow, J. Pouget-Abadie, M. Mirza, B. Xu, D. Warde-Farley, S. Ozair, A. Courville, and Y. Bengio, “Generative adversarial nets,” Jun. 2014.
- [10] T. Karras, T. Aila, S. Laine, and J. Lehtinen, “Progressive Growing of GANs for Improved Quality, Stability, and Variation,” Feb. 2018.
- [11] A. Dash, J. Ye, and G. Wang, “A review of generative adversarial networks (gans) and its applications in a wide variety of disciplines: from medical to remote sensing,” *IEEE Access*, 2023.
- [12] A. Creswell, T. White, V. Dumoulin, K. Arulkumaran, B. Sengupta, and A. A. Bharath, “Generative Adversarial Networks: An Overview,” *IEEE Signal Processing Magazine*, vol. 35, no. 1, pp. 53–65, Jan. 2018.
- [13] A. Radford, L. Metz, and S. Chintala, “Unsupervised Representation Learning with Deep Convolutional Generative Adversarial Networks,” Jan. 2016.
- [14] Z. Zheng, L. Zheng, and Y. Yang, “Unlabeled Samples Generated by GAN Improve the Person Re-identification Baseline in vitro,” Aug. 2017.
- [15] M. Frid-Adar, I. Diamant, E. Klang, M. Amitai, J. Goldberger, and H. Greenspan, “GAN-based Synthetic Medical Image Augmentation for increased CNN Performance in Liver Lesion Classification,” *Neurocomputing*, vol. 321, pp. 321–331, Dec. 2018.
- [16] J.-Y. Zhu, T. Park, P. Isola, and A. A. Efros, “Unpaired image-to-image translation using cycle-consistent adversarial networks,” in *Proceedings of the IEEE international conference on computer vision*, 2017, pp. 2223–2232.
- [17] Y. Hiasa, Y. Otake, M. Takao, T. Matsuo, K. Takashima, A. Carass, J. L. Prince, N. Sugano, and Y. Sato, “Cross-Modality Image Synthesis from Unpaired Data Using CycleGAN,” in *Simulation and Synthesis in Medical Imaging*, ser. Lecture Notes in Computer Science, A. Gooya, O. Goksel, I. Oguz, and N. Burgos, Eds. Cham: Springer International Publishing, 2018, pp. 31–41.
- [18] X. Zhu, Y. Liu, J. Li, T. Wan, and Z. Qin, “Emotion Classification with Data Augmentation Using Generative Adversarial Networks,” in *Advances in Knowledge Discovery and Data Mining*, ser. Lecture Notes in Computer Science, D. Phung, V. S. Tseng, G. I. Webb, B. Ho, M. Ganji, and L. Rashidi, Eds. Cham: Springer International Publishing, 2018, pp. 349–360.
- [19] T. Karras, S. Laine, and T. Aila, “A Style-Based Generator Architecture for Generative Adversarial Networks,” Mar. 2019.
- [20] K. Su, E. Zhou, X. Sun, C. Wang, D. Yu, and X. Luo, “Pre-trained StyleGAN Based Data Augmentation for Small Sample Brain CT Motion Artifacts Detection,” in *Advanced Data Mining and Applications*, ser. Lecture Notes in Computer Science, X. Yang, C.-D. Wang, M. S. Islam, and Z. Zhang, Eds. Cham: Springer International Publishing, 2020, pp. 339–346.
- [21] K. Wada and B. Chakraborty, “Performance Study of Image Data Augmentation by Generative Adversarial Networks,” in *2021 IEEE 12th Annual Information Technology, Electronics and Mobile Communication Conference (IEMCON)*, Oct. 2021, pp. 1022–1026.
- [22] T. Karras, M. Aittala, S. Laine, E. Härkönen, J. Hellsten, J. Lehtinen, and T. Aila, “Alias-free generative adversarial networks,” Oct. 2021.
- [23] F. Beuth, T. Schlosser, M. Friedrich, and D. Kowanko, “Improving Automated Visual Fault Detection by Combining a Biologically Plausible Model of Visual Attention with Deep Learning - Extended ArXiv Version,” *arXiv preprint arXiv:2102.06955*, pp. 1–15, 2021.
- [24] K. He, X. Zhang, S. Ren, and J. Sun, “Deep residual learning for image recognition,” in *Proceedings of the IEEE conference on computer vision and pattern recognition*, 2016, pp. 770–778.
- [25] T. Schlosser, M. Friedrich, and D. Kowanko, “Hexagonal image processing in the context of machine learning: Conception of a biologically inspired hexagonal deep learning framework,” in *2019 18th IEEE International Conference on Machine Learning and Applications (ICMLA)*. IEEE, 2019, pp. 1866–1873.